Molecular Cell, Volume *83*

Supplemental information

Structural snapshots of R-loop formation

by a type I-C CRISPR Cascade

Roisin E. O'Brien, Jack P.K. Bravo, Delisa Ramos, Grace N. Hibshman, Jacquelyn T. Wright, and David W. Taylor

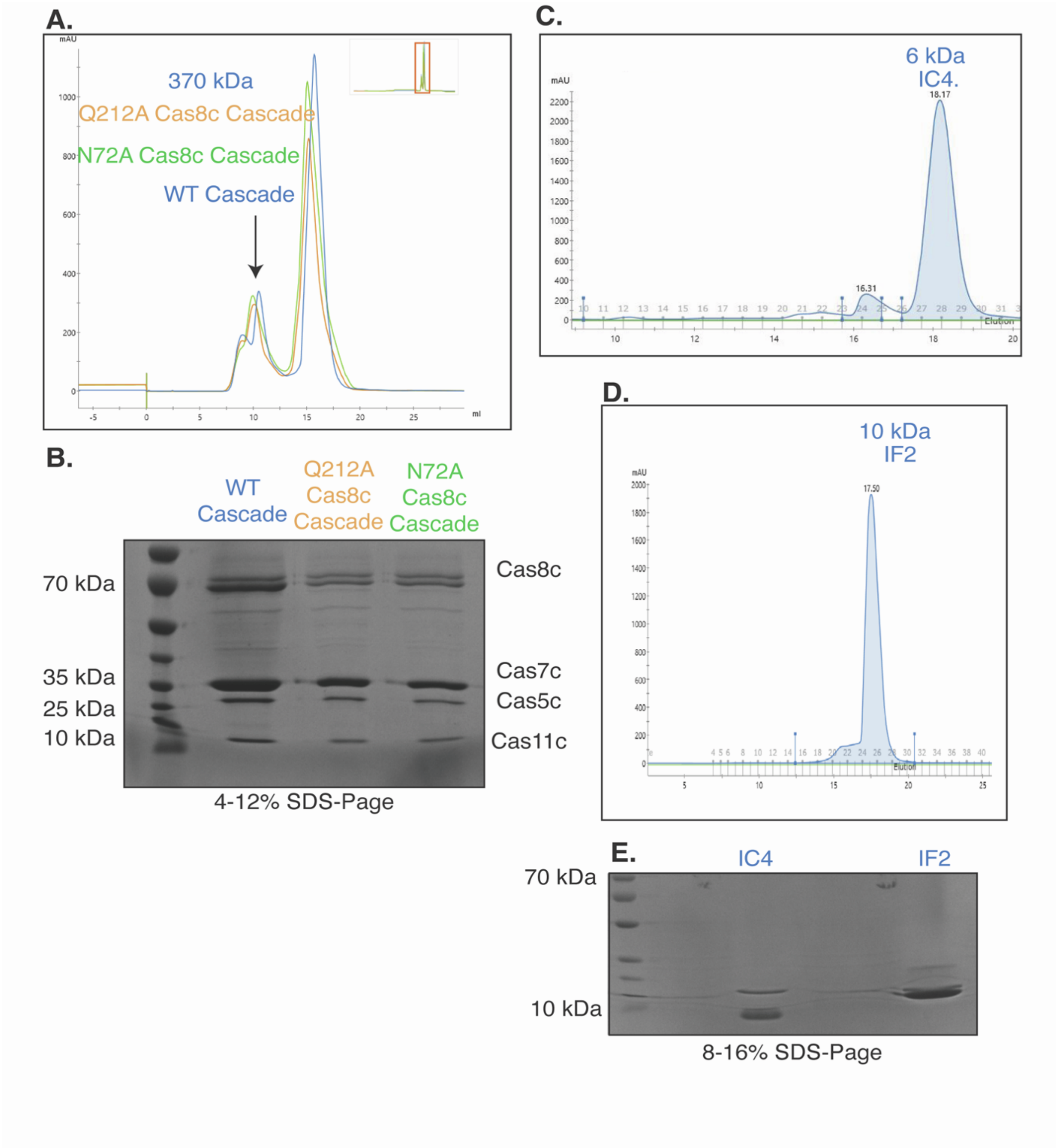

Figure S1. Related to Figures 1-5. Purification of the type I-C Cascade Cas8c mutant Cascade, AcrIF2 and AcrIC4. A,B. Size-exclusion chromatograph and SDS-Page analysis of WT, Cas8c-Q212A, and Cas8c-N72A Cascade. **C-E.** Size-exclusion chromatograph (C) and SDS-Page analysis of AcrIF2 and AcrIC4.

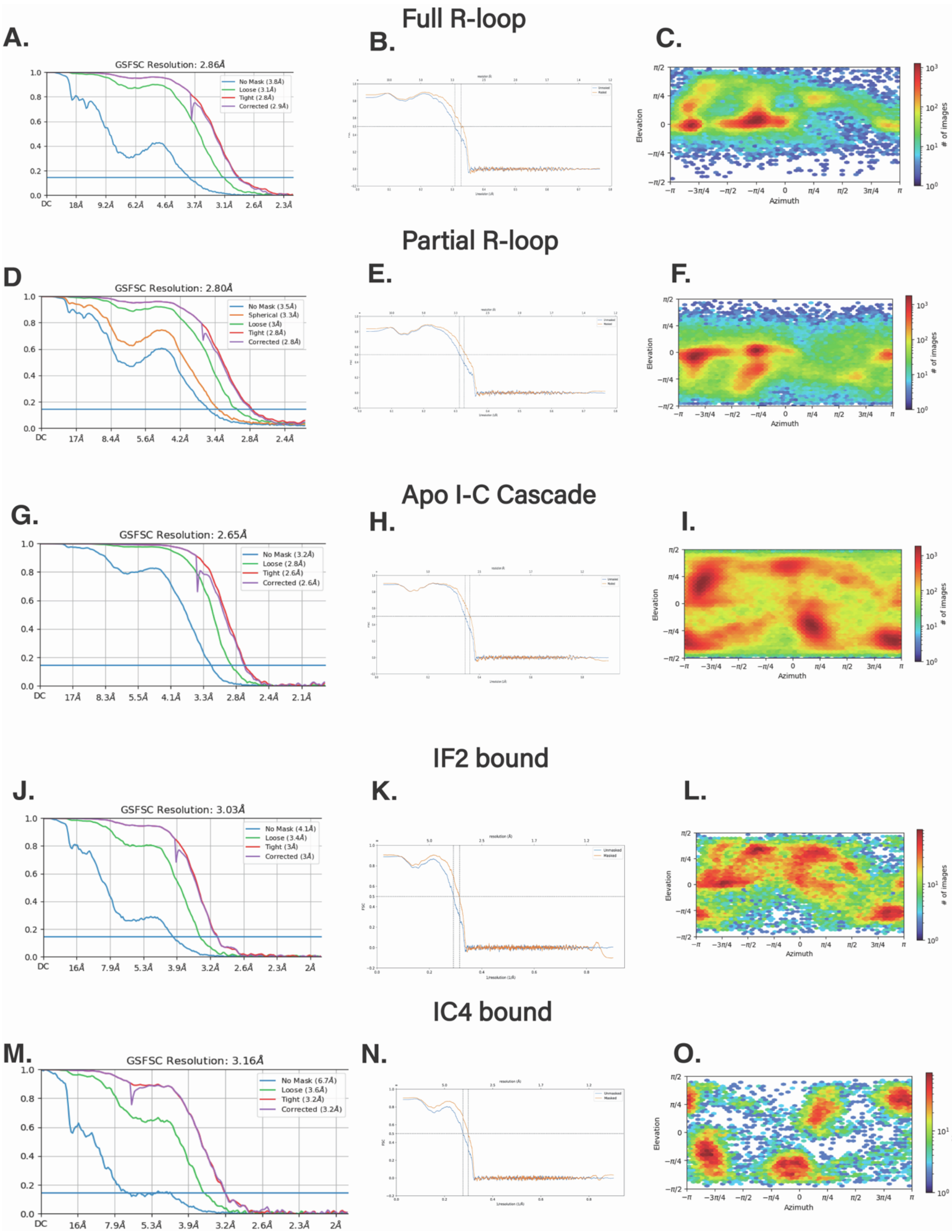

Figure S2. Related to Figure 1. Cryo-EM data analysis. **A.** Gold standard Fourier Shell Correlation (FSC) curves for type I-C Cascade bound to dsDNA complex. **B.** Map-to-model FSC for type I-C Cascade bound to dsDNA complex. **C.** Euler plot for type I-C Cascade bound to dsDNA complex **D**. Gold standard Fourier Shell Correlation (FSC) curves for type I-C Cascade partial R-loop complex. **E** Map-to-model FSC for type I-C Cascade partial R-loop complex **F.** Euler plot for type I-C Cascade partial R-loop. **G**. Gold standard Fourier Shell Correlation (FSC) curves for unbound type I-C Cascade. **H.** Map-to-model FSC for type I-C Cascade bound to unbound type I-C Cascade. **I**. Euler plot for unbound type I-C Cascade. **J**. Gold standard Fourier Shell Correlation (FSC) curves for type I-C Cascade bound to AcrIF2. **K.** Map-to-model FSC for type I-C Cascade for type I-C Cascade bound to AcrIF2. **L**. Euler plot for type I-C Cascade bound to AcrIF2. **M**. Gold standard Fourier Shell Correlation (FSC) curves for type I-C Cascade bound to AcrIC4. **N.** Map-to-model FSC for type I-C Cascade for type I-C Cascade bound to AcrIC4. **O**. Euler plot for type I-C Cascade bound to AcrIC4.

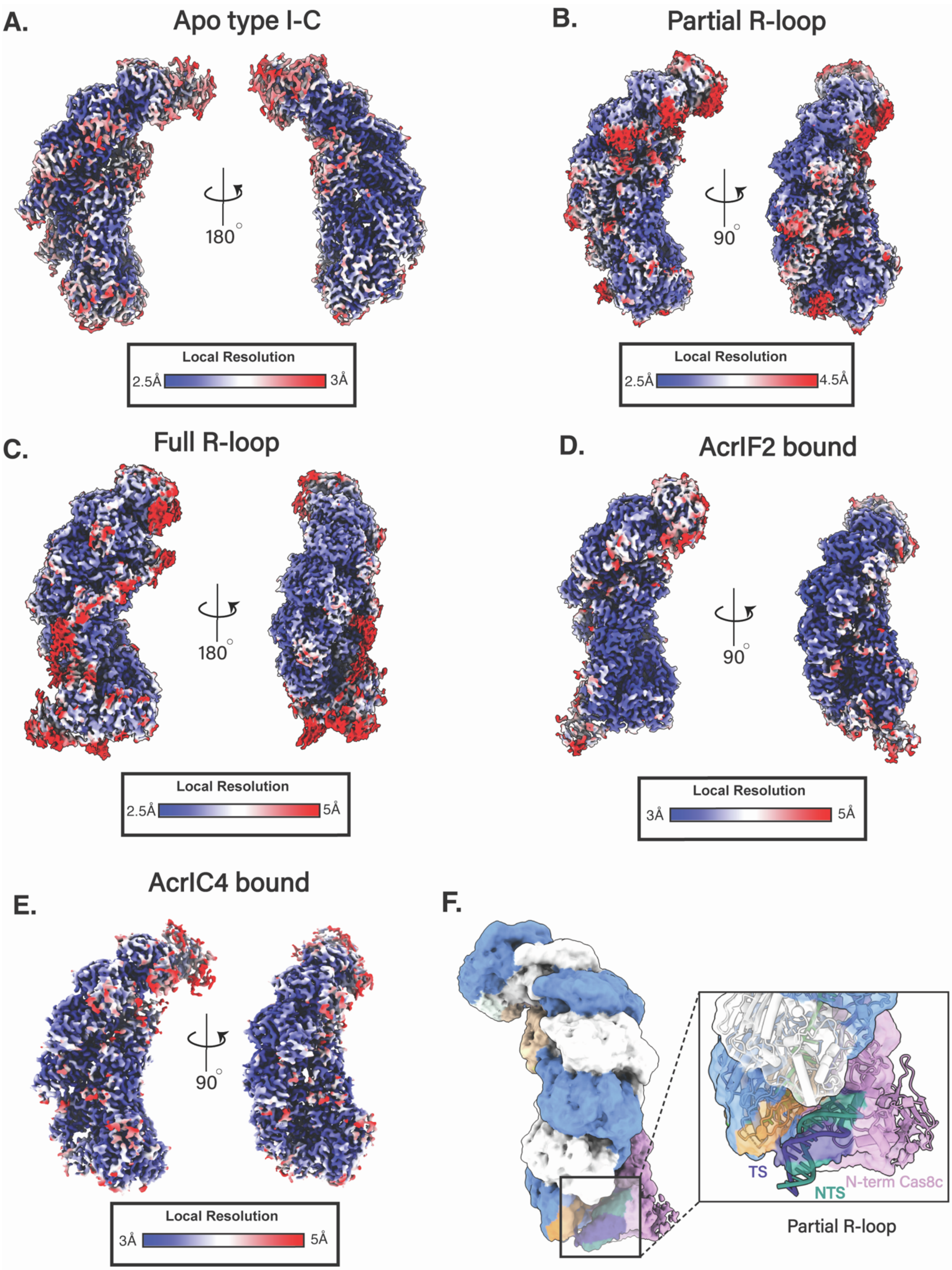

Figure S3. **Local resolution analysis. Related to Figures 1-5. A-E**. Sharpened maps colored according to local resolution. **F.** Cryo-EM density of partial R-loop structure.

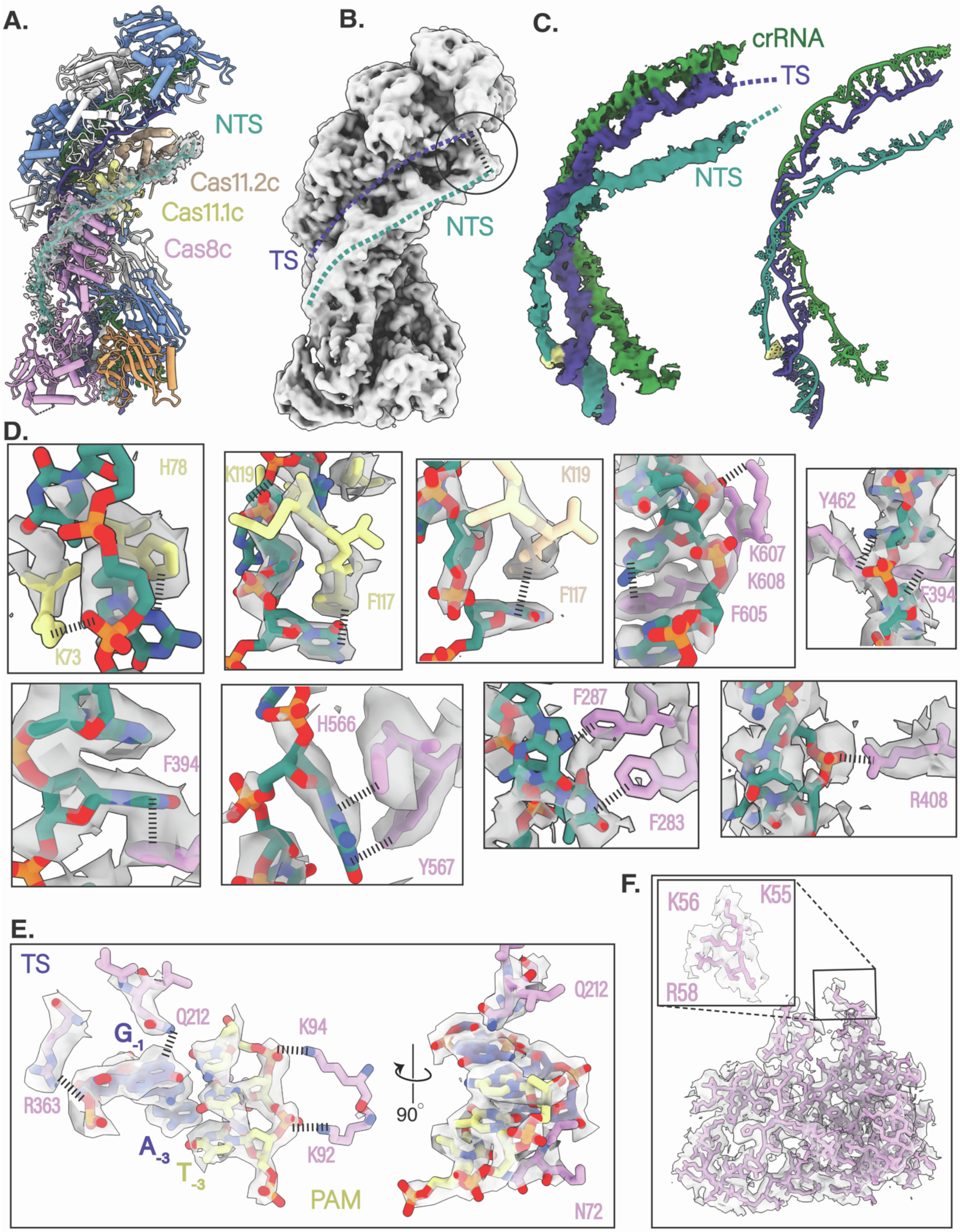

Figure S4. **Related to Figures 1-3. Representative cryo-EM densities. A.** NTS. **B.** NTS and TS reannealing at the top of the R-loop. **C.** NTS, TS, and crRNA densities and corresponding model **D.** NTS aromatic clamps and positively charged backbone stabilizing residues. **E.** PAM-recognition site **F.** Cas8c N-term.

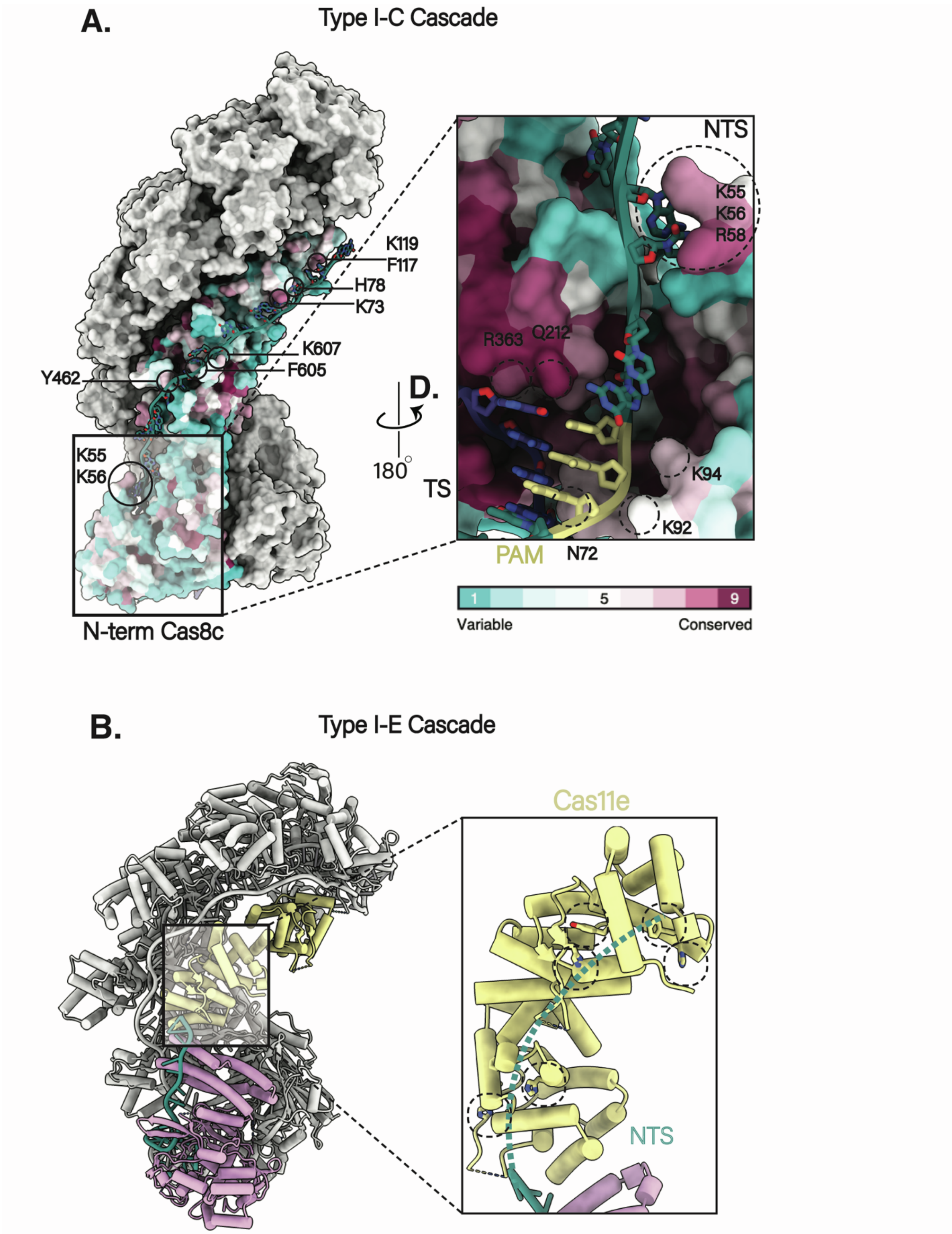

Figure S5. **Related to Figure 2. Conservation of NTS aromatic clamps across type I Cascades**. **A.** Aromatic and positively charged NTS stabilizing residues, and residues involved in PAM recognition (inset) are highly conserved across type I Cascades. **B.**

Multiple aromatic residues positioned along the putative NTS path (green) of type I-E Cascade [S1].

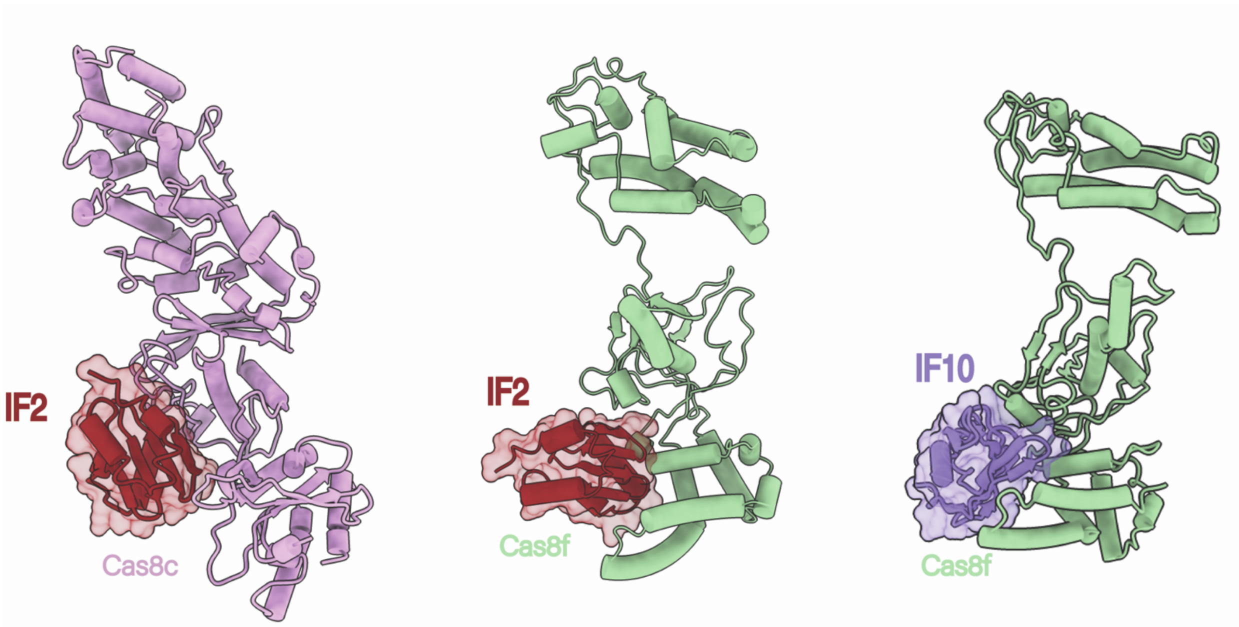

Figure S6. Related to Figures 4-5. Differences in positioning of Cas8 PAM blocking anti-CRISPRS. AcrIF2 inhibits both Cas8c and Cas8f through the same interface and at the same PAM site as AcrIF10, but at different orientations [S2, S3]**.**

Table S1. Related to Figure 1. Model Statistics for the type I-C Cascade structures.

	Type I-C apo model unbound	Type I-C Cascade full R-loop	Type I-C Cascade partial R-loop	Type I-C Cascade bound to AcrIF2	Type I-C Cascade bound to AcrIC4
Data collection and processing					
Voltage (kV)	200	300	300	200	200
Electron exposure (e–/Å^2)	40.5	80	80	40.5	40.5
Defocus range (μm)	1.5 to 2.5	1.2 to 2.2	1.2 to 2.2	1.5 to 2.5	1.5 to 2.5
Pixel size (Å)	0.94	1.1	1.1	0.94	0.94
Symmetry imposed	C1	C1	C1	C1	C1
Initial particle images (no.)	2 million	1.2 million	1.2 million	160,716	128,780
Final particle images (no.)	73,220	96,964	174,004	21,625	21,651
Map resolution (Å) FSC threshold	2.84 0.143	2.86 0.143	2.80 0.143	3.1 0.143	3.1 0.143
Map resolution range (Å)	N/A	N/A	N/A	N/A	N/A
Refinement					
Initial pdb model used	7KHA	7KHA	7KHA	7KHA 5UZ9	7KHA
Model resolution (Å) FSC threshold	2.8 0.5	3.1 0.5	3.1 0.5	3.2 0.5	3.4 0.5
Model resolution range (Å)	N/A	N/A	N/A	N/A	N/A
Map sharpening *B* factor (Å^2)	89.3	120.3	127.1	60.0	47.5
Model composition Non-hydrogen atoms Protein residues Ligands	 N/A 2855 48	 N/A 2975 135	 N/A 2855 64	 N/A 3082 48	 N/A 2912 45
B factors (Å^2) Protein Nucleotide	 00.00/101.82/37.11 00.0082.89/28.56	 00.00/136.69/53.34 12.60/223.93/96.73	 00.00/122.38/50.69 00.00/133.42/55.56	 16.24/186.4776.56 25.94/152.35/65.22	 31.17/224.86/92.39 46.22/141.66/82.27
R.m.s. deviations Bond lengths (Å) Bond angles (°)	 .0005 .706	 .003 .623	 .003 .682	 0.009 0.921	 0.003 0.646
Validation MolProbity score Clashscore Poor rotamers (%)	 1.68 4.92 1.71	 1.56 4.06 1.69	 1.71 6.01 1.25	 1.61 6.73 0.27	 1.75 9.49 0.00
Ramachandran plot Favored (%) Allowed (%) Disallowed (%)	 96.33 3.67 0.00	 96.82 3.18 0.00	 95.54 4.46 0.00	 96.37 3.63 0.00	 96.30 3.63 0.07

Table S2. Related to Figure 1. Plasmids used in this study.

Plasmid	Description	Reference
#81185	D*. vulgaris* type I-C Cascade for purification and cryo-EM studies	Addgene
#81186	D*. vulgaris* type I-C crRNA for co-expression with Cascade	Addgene
#89234	AcrIF2 for purification and cryo-EM studies	Addgene
pIF199	Backbone used for AcrIF2 and AcrIC4 for *in vivo* interference assay	Dillard et al [S4]
pIF412	Backbone used for dsDNA target for *in vivo* interference assay	Dillard et al [S4]
pIF385	Backbone used for Cascade-Cas3 for *in vivo* interference	Dillard et al [S4]
#48313	Backbone vector used for AcrIC4 for *in vivo* interference	Addgene
pRO01	Type I-C Cascade Cas8c mutant Q212A for purification and EMSA	This study
pRO02	Type I-C Cascade Cas8c mutant N72A for purification and EMSA	This study
pRO03	AcrIC4 for purification and cryo-EM studies	This study
#196399	pCDF-Duet1 vector with target sequence and 5' PAM for *in vivo* interference	Addgene This study
#196400	pBAD vector with IC cascade and cas3 for *in vivo* interference	Addgene This study
#196402	pET28b-Duet1 vector with Acr IF2 for *in vivo* interference	Addgene This study
#196403	pET28b-Duet1 vector with Acr-IC4 for *in vivo* interference	Addgene This study
pDR009	pBAD vector with IC Cascade and Cas3 with Cas8c N72A mutation for *in vivo* interference assay	This study
pDR010	pBAD vector with IC Cascade and Cas3 with Cas8c Q212A mutation for *in vivo* interference assay	This study
pDR011	pBAD vector with IC Cascade and Cas3 with Cas8c Aromatic mutants for *in vivo* interference assay	This study
pDR012	pBAD vector with IC Cascade and Cas3 with Cas8c Positive mutants for *in vivo* interference assay	This study
pDR013	pBAD vector with IC Cascade and Cas3 with Cas8c R363A/K94A/K92A mutants for *in vivo* interference assay	This study

Table S3. Related to Figures 1. Oligonucleotides used in this study.

Primer	Sequence (5' to 3')	Reference
roO1 Cas8c Q212A F	ggctGTTGCCTCGATAGTGTCCTTTAACAACAC	This study
roO2 Cas8c Q212A R	gctgcACCGCGAACGCCGTCTCG	This study
roO2 Cas8c N72A F	gggcATCAAACCGAACTTCCTG	This study
roO3 Cas8c N72A R	gccccCTTCTTTTCCGCGATAGG	This study
roO4 AcrIC4 F	TACTTCCAATCCAATGCAATGGACAATAAGATTACTCCT GCT	This study
roO5 AcrIC4 R	TTATCCACTTCCAATGTTATTAAGTTTCATCTCCACGCC A	This study
TS for cryo-EM experiments	AGCAGACTGGAGGAGTTTTCGCCATGCTCAGGCTGGC G AGTGCGCCACTCATCAAGCCATGTGGGCTGTCAAAAT	Hochstrasser et al [S5]
NTS for cryo-EM experiments and EMSA	AGCAGACTGGAGGAGTTTTCGCCATGCTCAGGCTGGC G AGTGCGCCACTCATCAAGCCATGTGGGCTGTCAAAAT	Hochstrasser et al [S5]
TS for EMSA	5' FAM- AGCAGACTGGAGGAGTTTTCGCCATGCTCAGGCTGGC G AGTGCGCCACTCATCAAGCCATGTGGGCTGTCAAAAT	Hochstrasser et al [S5]
dr001 pCDF-Duet1 vector with target sequence F	TTCGCCATGCTCAGGCTGGCGAGTGCGCCACTCATCA ACCTGTAGAAATAA TTTTGTTTAACTTTAAT	This study
dr002 pCDF-Duet1 vector with target sequence R	GGAATTGTTATCCGCTCAC	This study
iso020 pBAD vector with IC cascade-Cas3 F	GTTCGAAAAGTAAGAATTCGAAGCTTGG	This study
iso021 pBAD vector with IC cascade-Cas3 R	GCTGCAGATCTCGAGCTCGG	This study
iso063 pBAD vector with IC cascade-Cas3 F	CCATGGATCCGAGCTCGAGATCTGCAGCATGACACAT GGGGCTG	This study
iso064	CCAAGCTTCGAATTCTTACTTTTCGAACCTACAGCATCT CTTTGACCTC	This study

pBAD vector with IC cascade-Cas3 R		
dr007 pET28b-Duet1 vector with Acr IF2 F	GAAATAATTTTGTTTAACTTTAAGAAGGAGATATACCATGATGATCGCGCAACAGCATAA	This study
dr008 pET28b-Duet1 vector with Acr IF2 R	TACAGTATCCTTATGCTGTTGCGCGATCATCATGGTATATCTCCTTCTTAAAGTTAAACAA	This study
dr009 pET28b-Duet1 vector with Acr IF2 F	GAACGCCTGCTGGAGTCCGTAGAGGAGGAGCACCACCACCACCACCA	This study
dr010 pET28b-Duet1 vector with Acr IF2 R	CTTTGTTAGCAGCCGGATCTCAGTGGTGGTGGTGGTGGTGCTCCTCCTCTACGGACTCCA	This study
dr011 pET28b-Duet1 vector with Acr IF2 F	TGAGATCCGGCTGCTAAC	This study
dr012 pET28b-Duet1 vector with Acr IF2 R	CTCCTCCTCTACGGACTCC	This study
dr013 pET28b-Duet1 vector with Acr-IC4 F	TTTTGTTTAACTTTAAGAAGGAGATATACCATGGATAACAAAATCACACCTGCGGAC	This study
dr014 pET28b-Duet1 vector with Acr-IC4 R	GGTGTGATTTTGTTATCCATGGTATATCTCCTTCTTAAAGTTAAACAAAATTATTTCTAG	This study
dr015 pET28b-Duet1 vector with Acr-IC4 F	AAATATATTGAATGGCGTGGCGATGAAACGTGAGATCCGGCTGCTAA	This study
dr016 pET28b-Duet1 vector with Acr-IC4 R	CTTTCGGGCTTTGTTAGCAGCCGGATCTCACGTTTCATCGCCACGCCATTCAATATATTT	This study
dr017 pBAD vector with IC cascade-Cas3 F	GTAGAGGTCAAAGAGATGCTGTAGGTTCGAATGGCAAACTTGGCTGCTACTTTCGCTGAA	This study
dr018 pBAD vector with IC cascade-Cas3 R	GATGATGGTCGACGGCGCTATTGCTAACCAAACCTTCTGGCTGCCAAACTTC	This study
dr019 pBAD vector with IC cascade-Cas3 F	GAAGTTTGGCAGCCAGAAGGTTTGGTTAGCAATAGCGCCGTCGACCATCATC	This study

dr020 pBAD vector with IC cascade-Cas3 R	TTCAGCGAAAGTAGCAGCCAAGTTTGCCATTCGAACCT ACAGCATCTCTTTGACCTCTAC	This study
dr021 pBAD vector with IC cascade-Cas3 to anneal Cas8c gBlock insert F	AGCCATGACCGCCATTGCC	This study
dr022 pBAD vector with IC cascade-Cas3 to anneal Cas8c gBlock insert R	GCCCTCACCTCCGGTGAC	This study
dr023 Cas8c gBlocks insert F	CCCGTCGCGCACGTCACCGGAGGTGAGGGCATGATCC TGCAGGCATTGCATGG	This study
dr024 Cas8c Aromatic gBlock insert R	TCGTATCTGTTGGCAATGGCGGTCATGGCTAGTTCTCC TTGTTCTTCTTGGTCGCAA	This study
dr025 Cas8c Positive gBlock insert R	TCGTATCTGTTGGCAATGGCGGTCATGGCTAGTTCTCC TTGTTCGCCGCG	This study
dr026 Cas8c R363A/K92A/K94A gBlock insert R	TCGTATCTGTTGGCAATGGCGGTCATGGCTAGTTCTCC TTGTTCTTCTTGGTGAAAAGGG	This study

References

[S1] Hayes, R.P., Xiao, Y., Ding, F., van Erp, P.B.G., Rajashankar, K., Bailey, S., Wiedenheft, B., and Ke, A. (2016). Structural basis for promiscuous PAM recognition in type I-E Cascade from E. coli. Nature *530*, 499–503. 10.1038/nature16995.

[S2] Chowdhury, S., Carter, J., Rollins, M.F., Golden, S.M., Jackson, R.N., Hoffmann, C., Nosaka, L., Bondy-Denomy, J., Maxwell, K.L., Davidson, A.R., et al. (2017). Structure Reveals Mechanisms of Viral Suppressors that Intercept a CRISPR RNA-Guided Surveillance Complex. Cell *169*, 47-57.e11. 10.1016/j.cell.2017.03.012.

[S3] Guo, T.W., Bartesaghi, A., Yang, H., Falconieri, V., Rao, P., Merk, A., Eng, E.T., Raczkowski, A.M., Fox, T., Earl, L.A., et al. (2017). Cryo-EM Structures Reveal Mechanism and Inhibition of DNA Targeting by a CRISPR-Cas Surveillance Complex. Cell *171*, 414-426.e12. 10.1016/j.cell.2017.09.006.

[S4] Dillard, K.E., Brown, M.W., Johnson, N.V., Xiao, Y., Dolan, A., Hernandez, E., Dahlhauser, S.D., Kim, Y., Myler, L.R., Anslyn, E.V., et al. (2018). Assembly and Translocation of a CRISPR-Cas Primed Acquisition Complex. Cell *175*, 934-946.e15. 10.1016/j.cell.2018.09.039.

[S5] Hochstrasser, M.L., Taylor, D.W., Kornfeld, J.E., Nogales, E., and Doudna, J.A. (2016). DNA Targeting by a Minimal CRISPR RNA-Guided Cascade. Mol. Cell *63*, 840–851. 10.1016/j.molcel.2016.07.027.